HHS Public Access

Author manuscript

Behav Brain Res. Author manuscript; available in PMC 2016 October 15.

Published in final edited form as:

Behav Brain Res. 2015 October 15; 293: 18–26. doi:10.1016/j.bbr.2015.07.004.

Effects of an opioid (proenkephalin) polymorphism on neural response to errors in health and cocaine use disorder

Scott J. Moeller[1,2], **Nicasia Beebe-Wang**[4], **Kristin E. Schneider**[1], **Anna B. Konova**[5], **Muhammad A. Parvaz**[1,2], **Nelly Alia-Klein**[1,2], **Yasmin L. Hurd**[1,2,3], and **Rita Z. Goldstein**[1,2]

[1]Department of Psychiatry, Icahn School of Medicine at Mount Sinai, New York, NY 10029

[2]Department of Neuroscience, Icahn School of Medicine at Mount Sinai, New York, NY 10029

[3]Department of Pharmacology & Systems Therapeutics, Icahn School of Medicine at Mount Sinai, New York, NY 10029

[4]Department of Psychology, Harvard University, Cambridge, MA 02138

[5]Center for Neural Science, New York University, New York, NY 10003

Abstract

Chronic exposure to drugs of abuse perturbs the endogenous opioid system, which plays a critical role in the development and maintenance of addictive disorders. Opioid genetics may therefore play an important modulatory role in the expression of substance use disorders, but these genes have not been extensively characterized, especially in humans. In the current imaging genetics study, we investigated a single nucleotide polymorphism (SNP) of the protein-coding proenkephalin gene (*PENK*: rs2609997, recently shown to be associated with cannabis dependence) in 55 individuals with cocaine use disorder and 37 healthy controls. Analyses tested for *PENK* associations with fMRI response to error (during a classical color-word Stroop task) and gray matter volume (voxel-based morphometry) as a function of Diagnosis (cocaine, control). Results revealed whole-brain Diagnosis × *PENK* interactions on the neural response to errors (fMRI error>correct contrast) in the right putamen, left rostral anterior cingulate cortex/medial orbitofrontal cortex, and right inferior frontal gyrus; there was also a significant Diagnosis × *PENK* interaction on right inferior frontal gyrus gray matter volume. These interactions were driven by differences between individuals with cocaine use disorders and controls that were accentuated in individuals carrying the higher-risk *PENK* C-allele. Taken together, the *PENK* polymorphism – and potentially opioid neurotransmission more generally – modulates functioning and structural integrity of brain regions previously implicated in error-related processing. *PENK* could potentially render a subgroup of individuals with cocaine use disorder (i.e., C-allele carriers)

*Correspondence may be addressed to: Scott J. Moeller, One Gustave L. Levy Place, Box 1230, New York, NY 10029-6574; Tel: 212-241-6231; Fax: 212-803-6743; scott.moeller@mssm.edu. Correspondence may also be addressed to: Rita Z. Goldstein, One Gustave L. Levy Place, Box 1230, New York, NY 10029-6574; tel. (212) 824-9312; fax (212) 996-8931; rita.goldstein@mssm.edu.

Disclosure/Conflict of Interest

None declared.

more sensitive to mistakes or other related challenges; in future studies, these results could contribute to the development of individualized genetics-informed treatments.

Keywords

cocaine addiction; proenkephalin; error processing; functional magnetic resonance imaging; imaging genetics

1. INTRODUCTION

Error processing is a core executive function that allows for successful identification and correction of discrepancies between an intended and executed response [1, 2]. In health, the neural correlates of error-related processing typically encompass a network of regions of the medial prefrontal cortex (PFC) including the anterior cingulate cortex (ACC) [3–5]. Despite this common neural signature, error-related processing is also modulated by individual differences [6–9]. That is, certain individuals or groups may differ in the frequency with which they commit errors, and/or in the reactivity they show upon committing such errors. One important individual difference is the presence of a substance use disorder (SUD), a psychopathology marked by pervasive and disruptive neurocognitive disruptions (e.g., in error-related processing) that modulate the severity and course of the disease [10–19]. Our goal in the current study was to explore whether error-related processing in SUD is further modulated by another potentially important individual difference: opioid system genetics [specifically, a single nucleotide polymorphism (SNP) of the protein-coding proenkephalin gene (*PENK*: rs2609997)].

The opioid system forms a crucial component of the brain's reward circuit and importantly contributes to SUD symptomatology [20, 21]. Preclinical work has largely shown that knocking out proenkephalin – alone or in combination with related neuropeptides – reduces motivation, drug reward, and drug self-administration behavior [22–24]. In human SUD, opioid neurotransmission has been examined with positron emission tomography (PET). For example, [11C]carfentanil has been used to image mu opioid receptor binding in smokers [25–27], and in abusers of heroin [28], alcohol [29–31], and cocaine [32–35]. More proximally to the current goals, *PENK* gene variants that have a functional relationship with gene expression levels have been associated with increased risk for marijuana use disorder [36] and opioid use disorder [37, 38]. In contrast, *PENK* was not associated with alcohol dependence [39], and a postmortem study of alcohol-dependent individuals and controls did not reveal differences in *PENK* expression [40]. These studies collectively provide some suggestive evidence that *PENK* is associated with a substance abuse phenotype, highlighting this SNP as a potentially interesting candidate for further study. However, the specific role of the gene in SUD remains unclear.

Here, we used an imaging genetics approach to test for *PENK* associations with fMRI response to error (during a classical color-word Stroop task) and gray matter volume as a function of cocaine use disorder (CUD) diagnosis. The C-allele of *PENK* SNP rs2609997, associated with increased *PENK* expression compared with the T/T genotype, has been characterized as the "riskier" allele because of its association with increased negative

emotionality and a higher prevalence of cannabis abuse [36]. Nevertheless, because the literature on the functional effects of this particular *PENK* SNP – and, indeed, of *PENK* in general – is minimal, the findings of the current study can add crucial new information to the field by clarifying the neurobiological and psychological implications of carrying this C-allele. More specifically, uncovering this kind of intermediate imaging phenotype can provide important clues about this gene's operation vis-à-vis SUD [41]. Our decision to focus on CUD in the context of *PENK* was informed by prior research showing that *PENK* mRNA expression is impaired in monkeys that self-administered cocaine [42] and in humans who used cocaine [43], and that variants of this gene have been linked to other addictive disorders [36]. Our decision to focus on errors in the context of *PENK* was informed by prior research showing that *PENK* mRNA is expressed in limbic brain regions (e.g., amygdala) [36], relevant to a Stroop task insofar as these regions participate in the assigning of negative valence to errors and other negative action outcomes [44]. More importantly, *PENK* is also expressed in regions of the PFC [40, 45–48], of core relevance for performing Stroop tasks (recently reviewed in [49]). In the current study, participants performed an event-related color-word Stroop task while undergoing functional magnetic resonance imaging (fMRI) [50]; we have previously used this task to evaluate error-related processing in CUD [51–53]. During these same scanning sessions, structural MRI was also collected. We hypothesized that the "riskier" C-allele of the *PENK* SNP rs2609997 (i.e., compared with the less risky T/T genotype) (A) would be associated with more frequent and severe cocaine use; and (B) would accentuate group differences between CUD and controls in structure and responsiveness to error in limbic and PFC brain regions as indicated by significant whole-brain CUD × *PENK* interactions in these respective measures.

2. METHODS

2.1 Participants

Fifty-five CUD and 37 healthy controls, recruited through advertisements, local treatment facilities, and word of mouth, participated in this research; all provided written informed consent in accordance with the local Institutional Review Board. Some of these participants have been included in prior imaging genetics studies in our lab, but these studies have always included different genes and/or different neural probes, and accordingly have reported activations in different brain regions [54–56]. More specifically, we previously reported on polymorphisms of the dopamine transporter (*DAT1*) [54] and the protein-coding monoamine oxidase A gene (*MAOA*) [55, 56] while participants performed a *drug-word* inhibitory control task during fMRI [54], viewed unpleasant images during EEG [55], or simply while they underwent structural MRI scans [56]. For these reasons, overlap in variance with the current study is likely minimal. Exclusion criteria for the current study were: (A) history of head trauma or loss of consciousness (> 30 min) or other neurological disease of central origin (including seizures); (B) abnormal vital signs at time of screening; (C) history of major medical conditions, encompassing cardiovascular (including high blood pressure), endocrinological (including metabolic), oncological, or autoimmune diseases; (D) history of major psychiatric disorder, with some exceptions (for both groups: nicotine dependence; for CUD: comorbidities of known high co-occurrence including other SUD, major depression, and/or post-traumatic stress disorder [57, 58]); (E) pregnancy as

confirmed with a urine test in all females; (F) contraindications to the MRI environment; (G) except for cocaine in CUD participants, positive urine screens for psychoactive drugs or their metabolites (amphetamine or methamphetamine, phencyclidine, benzodiazepines, cannabis, opiates, barbiturates and inhalants) (note that although participants were permitted to have a current comorbid SUD as described below, participants who tested positive for other drugs indicating active use were excluded from all study procedures in the lab); (H) current evidence of intoxication from alcohol or any illicit drug. Protection against acute intoxication (alcohol and other drugs including cocaine) was afforded by our trained research staff, which has extensive experience with recognizing signs of intoxication in individuals with CUD (note that cigarette smoking was not restricted to avoid possible confounding effects on the fMRI results of cigarette withdrawal).

Participants underwent a comprehensive diagnostic interview, which consisted of: (A) Structured Clinical Interview for DSM-IV axis I Disorders [59]; (B) Addiction Severity Index [60], a semi-structured interview instrument used to assess history and severity of substance-related problems in seven problem areas (medical, employment, legal, alcohol, other drug use, family-social functioning, and psychological status); (C) Cocaine Selective Severity Assessment Scale [61], measuring cocaine abstinence/withdrawal signs and symptoms (i.e., sleep impairment, anxiety, energy levels, craving, and depressive symptoms) 24 hours within the time of interview; (D) Severity of Dependence Scale [62]; and (E) Cocaine Craving Questionnaire [63]. This interview identified the following cocaine-related diagnoses in CUD participants: current cocaine use disorder (N=43), cocaine use disorder in partial remission (N=8), and cocaine use disorder in full remission (N=4). Current Axis-I comorbidities were identified in 11 CUD participants, including marijuana use disorders (N=2), alcohol use disorders (N=5), ecstasy abuse (N=1), and major depression (N=1). Forty-two participants reported past comorbidities, including marijuana use disorder (N=27), alcohol use disorder (N=26), other stimulant use disorder (N=1), opiate (heroin) use disorder (N=2), phencyclidine use disorder (N=2), major depression (N=6), and post-traumatic stress disorder (N=2). Because all CUD participants indicated that cocaine was their primary drug of choice and/or that cocaine had led to their most severe substance-related consequences, other drug use disorders were considered as secondary to the cocaine diagnosis. Nevertheless, we controlled for histories of alcohol and cannabis use in follow-up analyses.

A subset of participants (12 CUD, 10 controls) was culled from a protocol that included administration of a dopaminergic partial agonist (methylphenidate) or counterbalanced placebo. In this case, the placebo data were used for the current analyses. Importantly, participants in this administration study were not overrepresented in any of the study groups (χ^2_3=3.99, p>0.26). Yet, we controlled for this procedural issue in follow-up analyses.

2.2 Genetics Screening

Participants' genotype was determined using an ABI 7900HT available at the Mount Sinai Quantitative PCR Shared Resource Facility, ascertained with whole blood samples. The chosen *PENK* SNP (rs2609997) was selected for inspection based principally on a prior study that linked this SNP to addictive behavior (cannabis dependence) in a fully independent sample of participants [36]. This SNP was also chosen based on pairwise

linkage disequilibrium (LD) relationships of an r^2 threshold of 0.8 and on haplotype data (www.hapmap.org) showing a minimum allele frequency of 0.10 in the population. The call rate was 100%, and the genotypes conformed to Hardy-Weinberg equilibrium. Following prior work [36], we partitioned the study participants into those with the T/T genotype versus C-allele carriers. C-allele carriers included 21 CUD and 15 controls, and T/T genotype included 34 CUD and 22 controls; analysis of the cross-tabulations did not reveal significant differences (χ^2_1=0.05, p>0.8). Demographic and drug use information on the current study sample, split by *PENK* and Diagnosis, are provided in Tables 1 and 2, respectively.

2.3 fMRI Procedures

Participants performed three runs of an event-related fMRI color-word Stroop task, with instructions to press for the ink color of color-words (red, blue, yellow, green) printed in their congruent or incongruent colors [50–53]. Each task run contained 12 incongruent events, totaling 36 such events per participant; there were 188 congruent events, totaling 564 such events. Participants committed an average of 28.7 ± 26.2 errors over the course of the task (i.e., summed across congruent and incongruent trials, and averaged across the 3 runs). No word or color of an incongruent stimulus mirrored the preceding congruent color-word; otherwise, stimuli were presented randomly. On each trial, a color word was presented for 1300 ms, which was also the time allotted for response (intertrial interval=350 ms); participants were not given performance feedback. Remuneration for task completion was $25 (fixed).

2.3.1 MRI Data Acquisition—MRI scanning was performed on a 4T whole-body Varian/Siemens MRI scanner. The blood-oxygenation-level-dependent (BOLD) fMRI responses were measured as a function of time using a T2*-weighted single-shot gradient-echo planar sequence (TE/TR=20/1600 ms, 3.125×3.125 mm^2 in-plane resolution, 4 mm slice thickness, 1 mm gap, typically 33 coronal slices, 20 cm FOV, 64 × 64 matrix size, 90°-flip angle, 200kHz bandwidth with ramp sampling, 207 time points, and 4 dummy scans to avoid non-equilibrium effects in the fMRI signal). Anatomical images were collected using a T1-weighted 3D-MDEFT (three-dimensional modified driven equilibrium Fourier transform) sequence [64] and a modified T2-weighted hyperecho sequence [65].

2.3.2 BOLD-fMRI Analyses—Image processing and analysis were performed with Statistical Parametric Mapping (SPM8) (Wellcome Trust Centre for Neuroimaging, London, UK). Echo-planar image reconstruction was performed using an iterative phase correction method that produces minimal signal-loss artifacts [66]. A six-parameter rigid body transformation (3 rotations, 3 translations) was used for image realignment and correction of head motion. Criteria for acceptable motion were 2 mm displacement and 2° rotation. All task runs from all participants meeting these motion criteria were included in the analyses (i.e., to maximize sample size in this imaging genetics study and similarly to our prior work [51, 52], we did not exclude participants listwise). The realigned datasets were spatially normalized to the standard Montreal Neurological Institute (MNI) stereotactic space using a 12-parameter affine transformation [67] and a voxel size of 3 × 3 × 3 mm. An 8-mm full-width-half-maximum Gaussian kernel spatially smoothed the data.

Two general linear models [68], which each included six motion regressors (3 translation and 3 rotation) and one task condition regressor convolved with a canonical hemodynamic response function and a high-pass filter (cut-off frequency: 1/90 s), were used to calculate individual BOLD-fMRI maps. Our primary design matrix of interest was constructed with one task regressor collapsed across both error trials (Congruent Incorrect and Incongruent Incorrect), leaving both correct trials (Congruent Correct and Incongruent Correct) to serve as the active, implicit baseline. Because the task contained mostly correct events, the beta weights for this incorrect (error) regressor reflected the variance to error events that remained after removing the variance related to correct events. Importantly, we have provided evidence that activations resulting from this design matrix reflect the error events, not the correct events [52]. Using this design matrix, we calculated a 1st Level contrast defined as (Incongruent Error + Congruent Error) – (Incongruent Correct + Congruent Correct). A secondary design matrix was constructed with one task regressor collapsed across both conflict trials (Incongruent Incorrect and Incongruent Correct), leaving both congruent trials (Congruent Incorrect and Congruent Correct) to serve as the implicit baseline. Using this second Design Matrix, we calculated a 1st Level contrast defined as (Incongruent Error + Incongruent Correct) – (Congruent Error + Congruent Correct).

At the 2nd Level, we conducted two whole-brain 2 (Diagnosis: CUD, control) × 2 (*PENK*: T/T vs. C/T or C/C) analyses of covariance (ANCOVA), one for each fMRI contrast, in SPM8; demographic variables that differed between the groups inclusive of race, smoking history, age, education, verbal IQ, and depression (Tables 1 and 2) were included in the models as covariates of no interest. We specified a height threshold of $p<0.005$ voxel-level uncorrected ($T=2.68$). We then used a Monte Carlo procedure [69], a program similar to AlphaSim, to identify the number of contiguous voxels necessary for a $p<0.05$ cluster-corrected threshold (i.e., given our imaging parameters and a height threshold of $T=2.68$), which was calculated to be 26 contiguous voxels [52]. Moreover, we applied additional statistical correction considering that we analyzed separate design matrices for incorrect>correct and incongruent>congruent; thus, we only report activations at a $p<0.01$ (rather than $p<0.05$) cluster-corrected threshold. The BOLD signals from significant clusters were extracted to inspect for outliers, for use in correlation analyses (see below), and to ensure that our main effects were not attributable to substance use histories of alcohol or marijuana (Tables 2) or to administration of a placebo pill [which occurred in a minority of participants (see above)]. For all analyses, anatomical specificity was corroborated using the AAL atlas in MRIcron. Note that because group differences between CUD and controls have been previously explored in this sample [51, 53], in the current study we only report *PENK* main effects and Diagnosis × *PENK* interactions.

2.3.3 Gray Matter Volume Analyses—Voxel-based morphometry (VBM) analysis was conducted with the VBM toolbox (VBM8) (Gaser, C, University of Jena, Department of Psychiatry, Germany; http://dbm.neuro.uni-jena.de/vbm/), which combines spatial normalization, tissue segmentation, and bias correction into a unified model. The MDEFT scans, which produce especially precise characterization of gray matter tissue [70], were first spatially normalized to standard proportional stereotaxic space (voxel size: 1 × 1 × 1 mm) and segmented into gray matter, white matter, and cerebrospinal fluid tissue classes

according to *a priori* tissue probability maps [71, 72]. A hidden Markov random field [73] maximized segmentation accuracy. Jacobian modulation compensated for the effect of spatial normalization and restored the original absolute gray matter volume in the gray matter segments. After smoothing the normalized and modulated gray matter segments with a 10 mm^3 full-width at half maximum Gaussian kernel, we again estimated a 2 (Diagnosis: CUD, control) × 2 (*PENK*: T/T vs. C/T or C/C) ANCOVA (with the same covariates of no interest as for the functional analyses). The number of contiguous voxels for significance was estimated to be 16 [69]; otherwise, the same statistical significance criteria as for the functional data were also applied for these analyses ($p<0.01$ cluster-corrected). Prior research has indeed revealed gray matter volume differences between CUD and controls [52, 74–76], and one study showed gray matter differences as a function of a different gene polymorphism (the monoamine oxidase A gene) [56].

2.3.4 Correlation Analyses—We first tested for functional-structural correspondence (correlations) between regions that showed parallel Diagnosis × *PENK* interactions for both methodologies. We then tested correlations between these functional activations or gray matter volume (i.e., limited to those activations that showed significant interactions) with behavior (task errors and reaction time) and current cocaine use frequency and severity (marked in Table 2). These correlations were conducted split by *PENK*; more exploratory correlations were also conducted to localize the source of any significant correlations that emerged (i.e., was a particular correlation driven by one diagnosis or significant across diagnoses?). Significance for all correlation analyses was set at $p<0.002$ to minimize Type I error (6 regions × 4 behavioral/drug use variables).

3. RESULTS

3.1 Associations with Disease Severity

In contrast to our first hypothesis, *PENK* was not associated with cocaine use frequency (days per week) or cocaine use severity (amount spent per use) within the CUD group (Table 2). The risk C-allele was also not more prevalent in CUD than controls.

3.2 Task Behavior

Our main interest in behavior was inspecting task errors, which were analyzed with a 2 (Diagnosis: CUD, control) × 2 (*PENK*: T/T, C-allele) × 2 (Trial: congruent, incongruent) mixed ANCOVA (that included all the same covariates as the SPM analyses). There were no main effects or interactions with *PENK*. We also examined reaction time, using a similar 2 × 2 × 2 mixed ANCOVA. This analysis revealed only a main effect of Trial [incongruent trials (891.8 ± 9.9 ms) > congruent (693.8 ± 7.0 ms) [$F(1,82)=8.69$, $p=0.004$], indicative of the reliable Stroop interference effect. Thus, neural effects of *PENK* (described below) are not attributable to group differences in task performance.

3.3 Color-Word Stroop (Table 3)

3.3.1 Error>Correct Activations—Main effects of *PENK* emerged in the superior frontal gyrus (C-allele>T/T genotype) and insula (T/T genotype>C-allele). Of greater interest, and supporting our second hypothesis, there were also Diagnosis × *PENK*

interactions to the error>correct contrast in the right putamen, left rostral ACC extending into medial orbitofrontal cortex (rACC/mOFC), and the right IFG extending to the middle frontal gyrus (dorsolateral prefrontal cortex). These interactions were driven by robust group differences between CUD participants and controls in individuals with the higher-risk *PENK* C-allele (in putamen and rACC/mOFC: reduced error-related activations in CUD; in IFG: increased error-related activations in CUD). These group differences were either absent (putamen, IFG) or reversed (rACC/mOFC) in individuals with the T/T genotype (Figure 1A–C).

3.3.2. Incongruent>Congruent Activations—For this fMRI contrast of the classical Stroop effect, there were no Diagnosis × *PENK* interactions; only main effects of *PENK* were observed. C-allele carriers showed greater activity to the incongruent>congruent contrast in the hippocampus, insula, postcentral gyrus, precentral gyrus, and supplementary motor area. Individuals with the T/T-genotype showed greater activity to this contrast in the cerebellum (vermis), middle/superior temporal gyrus, calcarine fissure, and bilateral thalamus. Given the lack of interactions with Diagnosis, these incongruent>congruent effects were not analyzed further.

3.4 Structure (Table 3)

A Diagnosis × *PENK* interaction emerged in the right IFG, showing the same pattern of effects as the functional right IFG effect during error (Figure 1D). Other interaction effects were limited to visual and auditory areas.

3.5 Brain-Behavior Correlations

Across all task- and drug use variables, only one correlation reached significance. In the T/T genotype, the higher the IFG fMRI response to error, the fewer total errors were committed during the task [$r(55)=-0.43$, $p=0.001$]; a subsequent follow-up analysis (for this effect only) showed that this correlation was driven by controls, although it did not reach nominal significance [$r(22)= -0.57$, $p=0.006$]. Nevertheless, these effects could indicate that in this less risky genotype, all participants (and particularly controls) performed the task better when this IFG response to error was enhanced. Because this direction of activation in this genotype characterized the healthy controls (Figure 1), this correlation suggests that activation of this region in this context may be adaptive. IFG structure and function did not correlate.

3.6 Other Substance Use History

We repeated the analyses above that reached significance (brain interactions and brain-behavior correlations) while (separately) controlling for history of alcohol use to intoxication, history of cannabis use, and placebo administration (through ANCOVAs or partial correlations as appropriate). Even when controlling for these variables, interactions were still detected across the whole sample in the putamen ($p<0.002$), rACC/mOFC ($p<0.004$), and IFG function ($p<0.055$ for cannabis; otherwise, $p<0.024$) and structure ($p<0.032$). The negative correlation between the number of errors and fMRI response to error in the IFG also remained significant ($p<0.001$). Thus, it is unlikely that our effects are

driven by histories of alcohol use or cannabis, or by the medication administration procedure.

4. DISCUSSION

The current study explored whether the *PENK* SNP rs2609997 (*PENK*) modulates brain function (error-related processing, assessed with fMRI BOLD during an event-related color-word Stroop task) and structure (gray matter integrity, assessed with VBM) in health and CUD. Although *PENK* did not directly associate with CUD severity (unsupportive of our first hypothesis), group differences between CUD and controls on the neural response to error and gray matter integrity were accentuated in individuals carrying the riskier C-allele of *PENK* (supporting our second hypothesis).

Our results collectively showed that *PENK* modulated the neural response to errors in largely anticipated regions. In particular, diagnosis × *PENK* interactions emerged during error-related processing in the rACC/mOFC, putamen, and IFG; and a similar Diagnosis × *PENK* interaction emerged in IFG gray matter volume. A consistent pattern in these interactions was a robust group difference between CUD participants and controls especially in the C-allele carriers; in the rACC/mOFC, there was also an opposite Diagnosis difference in those with the T/T genotype. The rACC is a core region involved in error-related processing even during emotionally-neutral cognitive tasks, implicated in generating the affective response that occurs shortly after error commission [77–79]; the rACC is also a main region of interest in PET studies probing the opioid system (e.g., [11C]carfentanil imaging of mu opioid receptors [80, 81]). Interestingly, in the current study the more dorsal component of the ACC was not identified, possibly indicating that *PENK* modulation may have impacted emotion rather than cognition. Other regions activated in our study such as the putamen and IFG, although not as consistently identified during error-related processing as the ACC, are indeed often reported as supporting this function [82–89]. Furthermore, the putamen forms part of a limbic striatal circuitry that, in addition to the amygdala, is expected to be modulated by *PENK* [36].

One interpretation of these findings is that lower error>correct rACC/mOFC and putamen response, in this case conferred by the C-allele of *PENK*, might render this CUD subgroup more insensitive to mistakes. It is unclear from the current data whether such putatively reduced error sensitivity conferred by *PENK* translates into increased drug-taking (i.e., rACC/mOFC activations did not correlate with drug use variables), but our prior research suggests that this hypothesis merits follow-up in future studies [52]. It is also possible that this CUD subgroup might have compensated with increased IFG response, enabling comparable performance/behavior to the other groups (and in agreement with the negative correlation between this region and errors). Although the mechanisms of these collective effects require further clarification in future studies – and accordingly the current results/conclusions should be interpreted with a degree of caution – our findings nonetheless support and justify additional investigation of this potentially interesting C-allele CUD subgroup.

Limitations of this study include the following. First, the sample size was relatively small for an imaging genetics approach. Importantly, however, all Diagnosis × *PENK* cells always contained at least 15 participants. Moreover, we observed a similar interaction pattern for the IFG across function and structure, strengthening confidence in these effects. We also leaned heavily on results of a prior study with a completely independent sample that examined this same gene [36]. Second, we were unable to examine homozygote carriers of the C-C genotype, who were scarce in our sample (N=2 across all available participants). If future studies can recruit C-C genotype participants, graded effects as a function of C-allele load could be inspected, similarly to research that has been conducted with the dopamine transporter gene [90–92]. Third, the study groups differed with respect to several demographic variables including race (Table 1), largely because assignment into genetic groupings did not reflect *a priori* recruitment; groups also differed with respect to multiple substance-related variables including use of cigarettes, alcohol, and marijuana (Table 2). For the former (demographics), results cannot be attributed to demographic covariates that differed between the groups because we controlled for these variables in the analyses. Further supporting this point, an exploratory examination of our main interaction effects in only African Americans showed that the average partial η^2 across the four interactions only dropped in magnitude from 0.098 to 0.077, suggesting that this variable (or the other demographics that differed between the groups) did not drive the results. Also note that we elected to use this covariation strategy instead of between-group matching, as our foremost priority was to maximize sample size for this study (i.e., in recognition of the first limitation). For the latter (drug use history), it is difficult to recruit healthy controls with the same levels of cigarette, alcohol, and cannabis use who do not also meet criteria for a SUD. Although we controlled for these variables in follow-up ANCOVAs/partial correlations, future work should aim to validate these findings using an active control group of substance-using but not dependent individuals. Fourth, we examined a single gene variant, and other genes could be involved in these effects. Importantly, however, the current study was conducted with firm *a priori* hypotheses regarding the impact of this *PENK* SNP on addictive disorders [36].

In conclusion, results of this study increase understanding of the *PENK* gene's modulation of brain structure and function in CUD. To our knowledge, this is one of the first studies to examine the functional correlates of this gene in human SUD – and the first to use functional neuroimaging for this purpose. This research augments work aiming to clarify the mechanisms underlying opioid genes' modulation of addictive disorders in humans [25, 26, 93] and of error-related processing more generally [94]. More importantly, our results suggest an intermediate phenotype that can increase understanding of the *PENK* gene's contribution to disease-relevant phenotypes such as SUD [41]. Investigation of the opioid system inclusive of the C-allele of *PENK* could ultimately aid in the development of individualized, genetics-informed treatments and medications in SUD that target specific deficits in this system. This approach could ultimately enable more appropriate and efficient allocation of scarce clinical resources and improved clinical outcomes in this difficult-to-treat psychopathology.

Acknowledgements

This study was supported by grants from the National Institute on Drug Abuse (to SJM: 1F32DA030017 and 1K01DA037452; to ABK: 5T32MH019524 Training in Systems and Integrative Neuroscience; to MAP: 1F32DA033088; to YLH: 1R01DA15446; to RZG: 1R01DA023579), and by the Mount Sinai Brain Imaging Center (BIC) (to SJM). We also gratefully acknowledge the contributions of Michail Misyrlis, Thomas Maloney, Patricia A. Woicik, Dardo Tomasi, Ruiliang Wang, and Gene-Jack Wang.

References

1. Taylor SF, Stern ER, Gehring WJ. Neural systems for error monitoring: Recent findings and theoretical perspectives. Neuroscientist. 2007; 13:160–172. [PubMed: 17404376]
2. Holroyd CB, Coles MG. The neural basis of human error processing: Reinforcement learning dopamine and the error-related negativity. Psychol Rev. 2002; 109:679–709. [PubMed: 12374324]
3. Manoach DS, Agam Y. Neural markers of errors as endophenotypes in neuropsychiatric disorders. Front Human Neurosci. 2013; 7:350.
4. Ridderinkhof KR, Ullsperger M, Crone EA, Nieuwenhuis S. The role of the medial frontal cortex in cognitive control. Science. 2004; 306:443–447. [PubMed: 15486290]
5. Hester R, Fassbender C, Garavan H. Individual differences in error processing: A review and reanalysis of three event-related fMRI studies using the GO/NOGO task. Cereb Cortex. 2004; 14:986–994. [PubMed: 15115734]
6. Rodehacke S, Mennigen E, Muller KU, Ripke S, Jacob MJ, Hubner T, Schmidt DH, Goschke T, Smolka MN. Interindividual differences in mid-adolescents in error monitoring and post-error adjustment. PLoS One. 2014; 9:88957.
7. van Noordt SJ, Segalowitz SJ. Performance monitoring and the medial prefrontal cortex: A review of individual differences and context effects as a window on self-regulation. Front Hum Neurosci. 2012; 6:197. [PubMed: 22798949]
8. Hoffmann S, Wascher E, Falkenstein M. Personality and error monitoring: An update. Front Hum Neurosci. 2012; 6:171. [PubMed: 22701417]
9. Sosic-Vasic Z, Ulrich M, Ruchsow M, Vasic N, Gron G. The modulating effect of personality traits on neural error monitoring: Evidence from event-related FMRI. PLoS One. 2012; 7:42930.
10. Garavan H, Hester R. The role of cognitive control in cocaine dependence. Neuropsychol Rev. 2007; 17:337–345. [PubMed: 17680368]
11. Woicik PA, Moeller SJ, Alia-Klein N, Maloney T, Lukasik TM, Yeliosof O, Wang GJ, Volkow ND, Goldstein RZ. The neuropsychology of cocaine addiction: Recent cocaine use masks impairment. Neuropsychopharmacology. 2009; 34:1112–1122. [PubMed: 18496524]
12. Hester R, Simões-Franklin C, Garavan H. Post-error behavior in active cocaine users: Poor awareness of errors in the presence of intact performance adjustments. Neuropsychopharmacology. 2007; 32:1974–1984. [PubMed: 17268406]
13. Hester R, Nestor L, Garavan H. Impaired error awareness and anterior cingulate cortex hypoactivity in chronic cannabis users. Neuropsychopharmacology. 2009; 34:2450–2458. [PubMed: 19553917]
14. Li CS, Huang C, Yan P, Bhagwagar Z, Milivojevic V, Sinha R. Neural correlates of impulse control during stop signal inhibition in cocaine-dependent men. Neuropsychopharmacology. 2008; 33:1798–1806. [PubMed: 17895916]
15. Connolly CG, Foxe JJ, Nierenberg J, Shpaner M, Garavan H. The neurobiology of cognitive control in successful cocaine abstinence. Drug Alcohol Depend. 2012; 121:45–53. [PubMed: 21885214]
16. Castelluccio BC, Meda SA, Muska CE, Stevens MC, Pearlson GD. Error processing in current and former cocaine users. Brain Imaging Behav. 2014; 8:87–96. [PubMed: 23949893]
17. Luijten M, Machielsen MW, Veltman DJ, Hester R, de Haan L, Franken IH. Systematic review of ERP and fMRI studies investigating inhibitory control and error processing in people with substance dependence and behavioural addictions. J Psychiatry Neurosci. 2014; 39:149–169. [PubMed: 24359877]

18. Goldstein RZ, Volkow ND. Dysfunction of the prefrontal cortex in addiction: Neuroimaging findings and clinical implications. Nat Rev Neurosci. 2011; 12:652–669. [PubMed: 22011681]
19. Goldstein RZ, Leskovjan AC, Hoff AL, Hitzemann R, Bashan F, Khalsa SS, Wang GJ, Fowler JS, Volkow ND. Severity of neuropsychological impairment in cocaine and alcohol addiction: Association with metabolism in the prefrontal cortex. Neuropsychologia. 2004; 42:1447–1458. [PubMed: 15246283]
20. Levran O, Yuferov V, Kreek MJ. The genetics of the opioid system and specific drug addictions. Hum Genet. 2012; 131:823–842. [PubMed: 22547174]
21. Trifilieff P, Martinez D. Kappa-opioid receptor signaling in the striatum as a potential modulator of dopamine transmission in cocaine dependence. Front Psychiatry. 2013; 4:44. [PubMed: 23760592]
22. Gutierrez-Cuesta J, Burokas A, Mancino S, Kummer S, Martin-Garcia E, Maldonado R. Effects of genetic deletion of endogenous opioid system components on the reinstatement of cocaine-seeking behavior in mice. Neuropsychopharmacology. 2014; 39:2974–2988. [PubMed: 24943644]
23. Tomasiewicz HC, Jacobs MM, Wilkinson MB, Wilson SP, Nestler EJ, Hurd YL. Proenkephalin mediates the enduring effects of adolescent cannabis exposure associated with adult opiate vulnerability. Biol Psychiatry. 2012; 72:803–810. [PubMed: 22683090]
24. Tseng A, Nguyen K, Hamid A, Garg M, Marquez P, Lutfy K. The role of endogenous beta-endorphin and enkephalins in ethanol reward. Neuropharmacology. 2013; 73:290–300. [PubMed: 23770261]
25. Domino EF, Hirasawa-Fujita M, Ni L, Guthrie SK, Zubieta JK. Regional brain [C]carfentanil binding following tobacco smoking. Prog Neuropsychopharmacol Biol Psychiatry. 2015; 59:100–104. [PubMed: 25598501]
26. Ray R, Ruparel K, Newberg A, Wileyto EP, Loughead JW, Divgi C, Blendy JA, Logan J, Zubieta JK, Lerman C. Human Mu Opioid Receptor (OPRM1 A118G) polymorphism is associated with brain mu-opioid receptor binding potential in smokers. Proc Natl Acad Sci U S A. 2011; 108:9268–9273. [PubMed: 21576462]
27. Scott DJ, Domino EF, Heitzeg MM, Koeppe RA, Ni L, Guthrie S, Zubieta JK. Smoking modulation of mu-opioid and dopamine D2 receptor-mediated neurotransmission in humans. Neuropsychopharmacology. 2007; 32:450–457. [PubMed: 17091130]
28. Zubieta J, Greenwald MK, Lombardi U, Woods JH, Kilbourn MR, Jewett DM, Koeppe RA, Schuster CR, Johanson CE. Buprenorphine-induced changes in mu-opioid receptor availability in male heroin-dependent volunteers: a preliminary study. Neuropsychopharmacology. 2000; 23:326–334. [PubMed: 10942856]
29. Bencherif B, Wand GS, McCaul ME, Kim YK, Ilgin N, Dannals RF, Frost JJ. Mu-opioid receptor binding measured by [11C]carfentanil positron emission tomography is related to craving and mood in alcohol dependence. Biol Psychiatry. 2004; 55:255–262. [PubMed: 14744466]
30. Weerts EM, Wand GS, Kuwabara H, Munro CA, Dannals RF, Hilton J, Frost JJ, McCaul ME. Positron emission tomography imaging of mu- and delta-opioid receptor binding in alcohol-dependent and healthy control subjects. Alcohol Clin Exp Res. 2011; 35:2162–2173. [PubMed: 21689118]
31. Weerts EM, Kim YK, Wand GS, Dannals RF, Lee JS, Frost JJ, McCaul ME. Differences in delta- and mu-opioid receptor blockade measured by positron emission tomography in naltrexone-treated recently abstinent alcohol-dependent subjects. Neuropsychopharmacology. 2008; 33:653–665. [PubMed: 17487229]
32. Zubieta JK, Gorelick DA, Stauffer R, Ravert HT, Dannals RF, Frost JJ. Increased mu opioid receptor binding detected by PET in cocaine-dependent men is associated with cocaine craving. Nat Med. 1996; 2:1225–1229. [PubMed: 8898749]
33. Ghitza UE, Preston KL, Epstein DH, Kuwabara H, Endres CJ, Bencherif B, Boyd SJ, Copersino ML, Frost JJ, Gorelick DA. Brain mu-opioid receptor binding predicts treatment outcome in cocaine-abusing outpatients. Biol Psychiatry. 2010; 68:697–703. [PubMed: 20579973]
34. Gorelick DA, Kim YK, Bencherif B, Boyd SJ, Nelson R, Copersino ML, Dannals RF, Frost JJ. Brain mu-opioid receptor binding: Relationship to relapse to cocaine use after monitored abstinence. Psychopharmacology (Berl). 2008; 200:475–486. [PubMed: 18762918]

35. Gorelick DA, Kim YK, Bencherif B, Boyd SJ, Nelson R, Copersino M, Endres CJ, Dannals RF, Frost JJ. Imaging brain mu-opioid receptors in abstinent cocaine users: Time course and relation to cocaine craving. Biol Psychiatry. 2005; 57:1573–1582. [PubMed: 15953495]
36. Jutras-Aswad D, Jacobs MM, Yiannoulos G, Roussos P, Bitsios P, Nomura Y, Liu X, Hurd YL. Cannabis-dependence risk relates to synergism between neuroticism and proenkephalin SNPs associated with amygdala gene expression: Case-control study. PLoS One. 2012; 7:39243.
37. Nikoshkov A, Drakenberg K, Wang X, Horvath MC, Keller E, Hurd YL. Opioid neuropeptide genotypes in relation to heroin abuse: Dopamine tone contributes to reversed mesolimbic proenkephalin expression. Proc Natl Acad Sci U S A. 2008; 105:786–791. [PubMed: 18184800]
38. Comings DE, Blake H, Dietz G, Gade-Andavolu R, Legro RS, Saucier G, Johnson P, Verde R, MacMurray JP. The proenkephalin gene (PENK) and opioid dependence. Neuroreport. 1999; 10:1133–1135. [PubMed: 10321497]
39. Chan RJ, McBride AW, Thomasson HR, Ykenney A, Crabb DW. Allele frequencies of the preproenkephalin A (PENK) gene CArepeat in Asians African-Americans and Caucasians: Lack of evidence for different allele frequencies in alcoholics. Alcohol Clin Exp Res. 1994; 18:533–535. [PubMed: 7943650]
40. Bazov I, Kononenko O, Watanabe H, Kuntic V, Sarkisyan D, Taqi MM, Hussain MZ, Nyberg F, Yakovleva T, Bakalkin G. The endogenous opioid system in human alcoholics: Molecular adaptations in brain areas involved in cognitive control of addiction. Addict Biol. 2013; 18:161–169. [PubMed: 21955155]
41. Flint J, Timpson N, Munafo M. Assessing the utility of intermediate phenotypes for genetic mapping of psychiatric disease. Trends Neurosci. 2014; 37:733–741. [PubMed: 25216981]
42. Daunais JB, Nader MA, Porrino LJ. Long-term cocaine self-administration decreases striatal preproenkephalin mRNA in rhesus monkeys. Pharmacol Biochem Behav. 1997; 57:471–475. [PubMed: 9218271]
43. Hurd YL, Herkenham M. Molecular alterations in the neostriatum of human cocaine addicts. Synapse. 1993; 13:357–369. [PubMed: 7683144]
44. Koban L, Pourtois G. Brain systems underlying the affective and social monitoring of actions: An integrative review. Neurosci Biobehav Rev. 2014; 46P1:71–84. [PubMed: 24681006]
45. Mendez M, Morales-Mulia M. Ethanol exposure differentially alters pro-enkephalin mRNA expression in regions of the mesocorticolimbic system. Psychopharmacology (Berl). 2006; 189:117–124. [PubMed: 17047937]
46. Marinelli PW, Kiianmaa K, Gianoulakis C. Opioid propeptide mRNA content and receptor density in the brains of AA and ANA rats. Life Sci. 2000; 66:1915–1927. [PubMed: 10821116]
47. Morales-Mulia M, Panayi F, Lambas-Senas L, Scarna H, Mendez M. Changes in Proenkephalin mRNA expression in forebrain areas after amphetamine-induced behavioural sensitization. Pharmacol Biochem Behav. 2007; 87:232–240. [PubMed: 17537495]
48. Volk DW, Radchenkova PV, Walker EM, Sengupta EJ, Lewis DA. Cortical opioid markers in schizophrenia and across postnatal development. Cereb Cortex. 2012; 22:1215–1223. [PubMed: 21810780]
49. Cieslik EC, Mueller VI, Eickhoff CR, Langner R, Eickhoff SB. Three key regions for supervisory attentional control: Evidence from neuroimaging meta-analyses. Neurosci Biobehav Rev. 2015; 48C:22–34. [PubMed: 25446951]
50. Leung HC, Skudlarski P, Gatenby JC, Peterson BS, Gore JC. An event-related functional MRI study of the stroop color word interference task. Cereb Cortex. 2000; 10:552–560. [PubMed: 10859133]
51. Moeller SJ, Honorio J, Tomasi D, Parvaz MA, Woicik PA, Volkow ND, Goldstein RZ. Methylphenidate enhances executive function and optimizes prefrontal function in both health and cocaine addiction. Cereb Cortex. 2014; 24:643–653. [PubMed: 23162047]
52. Moeller SJ, Konova AB, Parvaz MA, Tomasi D, Lane RD, Fort C, Goldstein RZ. Functional structural and emotional correlates of impaired insight in cocaine addiction. JAMA Psychiatry. 2014; 71:61–70. [PubMed: 24258223]
53. Moeller SJ, Tomasi D, Honorio J, Volkow ND, Goldstein RZ. Dopaminergic involvement during mental fatigue in health and cocaine addiction. Transl Psychiatry. 2012; 2:176.

54. Moeller SJ, Parvaz MA, Shumay E, Beebe-Wang N, Konova AB, Alia-Klein N, Volkow ND, Goldstein RZ. Gene x abstinence effects on drug cue reactivity in addiction: Multimodal evidence. J Neurosci. 2013; 33:10027–10036. [PubMed: 23761898]
55. Moeller SJ, Parvaz MA, Shumay E, Wu S, Beebe-Wang N, Konova AB, Misyrlis M, Alia-Klein N, Goldstein RZ. Monoamine polygenic liability in health and cocaine dependence: Imaging genetics study of aversive processing and associations with depression symptomatology. Drug Alcohol Depend. 2014; 140:17–24. [PubMed: 24837582]
56. Alia-Klein N, Parvaz MA, Woicik PA, Konova AB, Maloney T, Shumay E, Wang R, Telang F, Biegon A, Wang GJ, Fowler JS, Tomasi D, Volkow ND, Goldstein RZ. Gene x disease interaction on orbitofrontal gray matter in cocaine addiction. Arch Gen Psychiatry. 2011; 68:283–294. [PubMed: 21383264]
57. Rounsaville BJ, Anton SF, Carroll K, Budde D. Psychiatric diagnoses of treatment-seeking cocaine abusers. Arch Gen Psychiatry. 1991; 48:43–51. [PubMed: 1984761]
58. Narvaez JC, Jansen K, Pinheiro RT, Kapczinski F, Silva RA, Pechansky F, Magalhaes PV. Psychiatric and substance-use comorbidities associated with lifetime crack cocaine use in young adults in the general population. Compr Psychiatry. 2014; 55:1369–1376. [PubMed: 24933652]
59. First, MB.; Spitzer, RL.; Gibbon, M.; Williams, J.; Williams, J. Biometrics Research Department. New York: New York State Psychiatric Institute; 1996. Structured clinical interview for DSM-IV axis I disorders - patient edition (SCID-I/P, Version 2.0).
60. McLellan AT, Kushner H, Metzger D, Peters R, Smith I, Grissom G, Pettinati H, Argeriou M. The fifth edition of the Addiction Severity Index. J Subst Abuse Treat. 1992; 9:199–213. [PubMed: 1334156]
61. Kampman KM, Volpicelli JR, McGinnis DE, Alterman AI, Weinrieb RM, D'Angelo L, Epperson LE. Reliability and validity of the Cocaine Selective Severity Assessment. Addict Behav. 1998; 23:449–461. [PubMed: 9698974]
62. Gossop M, Griffiths P, Powis B, Strang J. Severity of dependence route of administration of heroin cocaine and amphetamines. Br J Addict. 1992; 87:1527–1536. [PubMed: 1458032]
63. Tiffany ST, Singleton E, Haertzen CA, Henningfield JE. The development of a cocaine craving questionnaire. Drug Alcohol Depend. 1993; 34:19–28. [PubMed: 8174499]
64. Lee JH, Garwood M, Menon R, Adriany G, Andersen P, Truwit CL, Ugurbil K. High contrast and fast three-dimensional magnetic resonance imaging at high fields. Magn Reson Med. 1995; 34:308–312. [PubMed: 7500867]
65. Hennig J, Scheffler K. Hyperechoes. Magn Reson Med. 2001; 46:6–12. [PubMed: 11443704]
66. Caparelli E, Tomasi D. K-space spatial low-pass filters can increase signal loss artifacts in Echo-Planar Imaging. Biomed Signal Process Control. 2008; 3:107–114. [PubMed: 19122745]
67. Ashburner J, Neelin P, Collins DL, Evans A, Friston K. Incorporating prior knowledge into image registration. Neuroimage. 1997; 6:344–352. [PubMed: 9417976]
68. Friston KJ, Holmes AP, Worsley KJ, Poline JB, Frith CD, Frackowiak RS. Statistical parametric maps in functional imaging: A general approach. Hum Brain Mapp. 1995; 2:189–210.
69. Slotnick SD, Moo LR, Segal JB, Hart J. Distinct prefrontal cortex activity associated with item memory and source for visual shapes. Brain Res Cogn Brain Res. 2003; 17:75–82. [PubMed: 12763194]
70. Tardif CL, Collins DL, Pike GB. Sensitivity of voxel-based morphometry analysis to choice of imaging protocol at 3 T. Neuroimage. 2009; 44:827–838. [PubMed: 18996205]
71. Ashburner J, Friston KJ. Voxel-based morphometry--the methods. Neuroimage. 2000; 11:805–821. [PubMed: 10860804]
72. Ashburner J, Friston KJ. Unified segmentation. Neuroimage. 2005; 26:839–851. [PubMed: 15955494]
73. Cuadra MB, Cammoun L, Butz T, Cuisenaire O, Thiran JP. Comparison and validation of tissue modelization and statistical classification methods in T1-weighted MR brain images. IEEE Trans Med Imaging. 2005; 24:1548–1565. [PubMed: 16350916]
74. Franklin TR, Acton PD, Maldjian JA, Gray JD, Croft JR, Dackis CA, O'Brien CP, Childress AR. Decreased gray matter concentration in the insular orbitofrontal, cingulate and temporal cortices of cocaine patients. Biol Psychiatry. 2002; 51:134–142. [PubMed: 11822992]

75. Matochik JA, London ED, Eldreth DA, Cadet JL, Bolla KI. Frontal cortical tissue composition in abstinent cocaine abusers: A magnetic resonance imaging study. Neuroimage. 2003; 19:1095–1102. [PubMed: 12880835]
76. Konova AB, Moeller SJ, Tomasi D, Parvaz MA, Alia-Klein N, Volkow ND, Goldstein RZ. Structural and behavioral correlates of abnormal encoding of money value in the sensorimotor striatum in cocaine addiction. Eur J Neurosci. 2012; 36:2979–2988. [PubMed: 22775285]
77. Kiehl KA, Smith AM, Hare RD, Mendrek A, Forster BB, Brink J, Liddle PF. Limbic abnormalities in affective processing by criminal psychopaths as revealed by functional magnetic resonance imaging. Biol Psychiatry. 2001; 50:677–684. [PubMed: 11704074]
78. Braver TS, Barch DM, Gray JR, Molfese DL, Snyder A. Anterior cingulate cortex response conflict: effects of frequency inhibition and errors. Cereb Cortex. 2001; 11:825–836. [PubMed: 11532888]
79. Edwards BG, Calhoun VD, Kiehl KA. Joint ICA of ERP and fMRI during error-monitoring. Neuroimage. 2012; 59:1896–1903. [PubMed: 21930218]
80. Wager TD, Scott DJ, Zubieta JK. Placebo effects on human mu-opioid activity during pain. Proc Natl Acad Sci U S A. 2007; 104:11056–11061. [PubMed: 17578917]
81. Zubieta JK, Ketter TA, Bueller JA, Xu Y, Kilbourn MR, Young EA, Koeppe RA. Regulation of human affective responses by anterior cingulate and limbic mu-opioid neurotransmission. Arch Gen Psychiatry. 2003; 60:1145–1153. [PubMed: 14609890]
82. Garavan H, Ross TJ, Murphy K, Roche RA, Stein EA. Dissociable executive functions in the dynamic control of behavior: inhibition error detection and correction. Neuroimage. 2002; 17:1820–1829. [PubMed: 12498755]
83. Spunt RP, Lieberman MD, Cohen JR, Eisenberger NI. The phenomenology of error processing: The dorsal ACC response to stop-signal errors tracks reports of negative affect. J Cogn Neurosci. 2012; 24:1753–1765. [PubMed: 22571460]
84. Stewart JL, Parnass JM, May AC, Davenport PW, Paulus MP. Altered frontocingulate activation during aversive interoceptive processing in young adults transitioning to problem stimulant use. Front Syst Neurosci. 2013; 7:89. [PubMed: 24298242]
85. Stevens MC, Kiehl KA, Pearlson GD, Calhoun VD. Brain network dynamics during error commission. Hum Brain Mapp. 2009; 30:24–37. [PubMed: 17979124]
86. Donamayor N, Heilbronner U, Munte TF. Coupling electrophysiological and hemodynamic responses to errors. Hum Brain Mapp. 2012; 33:1621–1633. [PubMed: 21618663]
87. Schaeffer DJ, Amlung MT, Li Q, Krafft CE, Austin BP, Dyckman KA, McDowell JE. Neural correlates of behavioral variation in healthy adults' antisaccade performance. Psychophysiology. 2013; 50:325–333. [PubMed: 23418930]
88. Claus ED, Feldstein Ewing SW, Filbey FM, Hutchison KE. Behavioral control in alcohol use disorders: Relationships with severity. J Stud Alcohol Drugs. 2013; 74:141–151. [PubMed: 23200160]
89. Costa A, Riedel M, Pogarell O, Menzel-Zelnitschek F, Schwarz M, Reiser M, Moller HJ, Rubia K, Meindl T, Ettinger U. Methylphenidate effects on neural activity during response inhibition in healthy humans. Cereb Cortex. 2013; 23:1179–1189. [PubMed: 22581848]
90. Lott DC, Kim SJ, Cook EH Jr, de Wit H. Dopamine transporter gene associated with diminished subjective response to amphetamine. Neuropsychopharmacology. 2005; 30:602–609. [PubMed: 15602501]
91. Stein MA, Waldman ID, Sarampote CS, Seymour KE, Robb AS, Conlon C, Kim SJ, Cook EH. Dopamine transporter genotype and methylphenidate dose response in children with ADHD. Neuropsychopharmacology. 2005; 30:1374–1382. [PubMed: 15827573]
92. den Ouden HE, Daw ND, Fernandez G, Elshout JA, Rijpkema M, Hoogman M, Franke B, Cools R. Dissociable effects of dopamine and serotonin on reversal learning. Neuron. 2013; 80:1090–1100. [PubMed: 24267657]
93. Xu K, Seo D, Hodgkinson C, Hu Y, Goldman D, Sinha R. A variant on the kappa opioid receptor gene (OPRK1) is associated with stress response related drug craving limbic brain activation and cocaine relapse risk. Transl Psychiatry. 2013; 3:292.

94. Agam Y, Vangel M, Roffman JL, Gallagher PJ, Chaponis J, Haddad S, Goff DC, Greenberg JL, Wilhelm S, Smoller JW, Manoach DS. Dissociable genetic contributions to error processing: a multimodal neuroimaging study. PLoS One. 2014; 9:101784.

95. Wechsler, D. Wechsler abbreviated scale of intelligence. San Antonio, TX: Psychological Corporation; 1999.

96. Wilkinson, G. The Wide-Range Achievement Test 3- Administration Manual. Wilmington, DE: Wide Range Inc; 1993.

97. Beck AT. The Beck Depression Inventory (BDI-II). The Psychological Corporation. 1996 DOI.

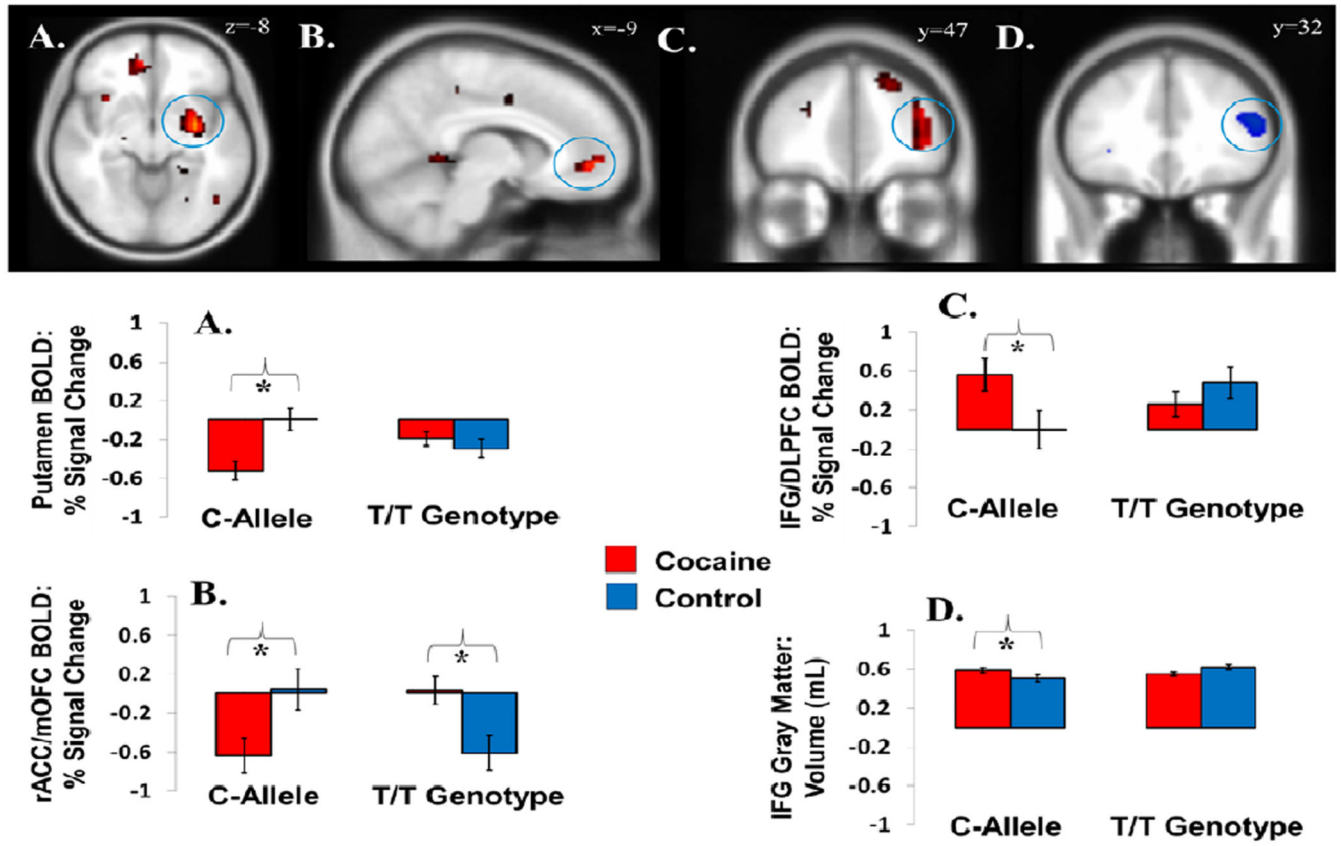

Figure 1.

PENK × Diagnosis effects on brain function and structure. During an event-related fMRI Stroop task, interactions for the fMRI contrast error>correct were observed in the (A) putamen, (B) rostral anterior cingulate cortex extending to the medial orbitofrontal cortex (rACC/mOFC), and (C) inferior frontal gyrus/dorsolateral prefrontal cortex. For all regions, these interactions were at least partially driven by a more pronounced difference between ocaine abusers and controls in individuals carrying the “riskier” C-allele. (D) As assessed with voxel-based morphometry (VBM), there was a similar *PENK* × Diagnosis interaction on IFG gray matter volume, again such that differences between cocaine abusers and controls were accentuated in C-allele carriers. All images are displayed in neurological convention; for display purposes only, they are thresholded at $2.0 \leq T \leq 5.0$. Functional effects are in red shades; structural effects are in blue shades.

Table 1

Demographics of all study participants.

		PENK: C-Allele Carrier		*PENK*: T/T Genotype	
	Between-Group Test	**Cocaine (n = 21)**	**Control (n =15)**	**Cocaine (n = 34)**	**Control (n = 22)**
Gender, male/female	$\chi^2_3 = 0.79$	19/2	13/2	30/4	18/4
Ethnicity, black/white/other	$\chi^2_6 = 20.42^{**}$	$9/7/5^{c,d}$	$8/5/2^{c}$	$31/3/0^{a,b}$	$18/3/1^{a}$
Education, years	$F_{3,88} = 3.73^{*}$	13.2 ± 1.9^{c}	13.0 ± 1.8	12.5 ± 1.4^{ab}	14.0 ± 1.9^{c}
Age, years	$F_{3,88} = 2.98^{*}$	41.4 ± 8.0	41.0 ± 7.7	45.0 ± 5.6^{d}	39.8 ± 7.4^{c}
Nonverbal Intelligence: Wechsler Abbreviated Scale of Intelligence: Matrix Reasoning scaled score [95]	$F_{3,87} = 2.51$	10.6 ± 2.5	11.8 ± 2.4	9.4 ± 3.1	10.0 ± 3.3
Verbal IQ: Wide Range Achievement Test III: grade equivalent score [96]	$F_{3,87} = 5.93^{**}$	12.3 ± 1.1^{c}	11.5 ± 3.2^{c}	$9.5 \pm 3.5^{a,b,d}$	11.8 ± 2.2^{c}
Self-reported state depression (Beck Depression Inventory) [97]	$F_{3,88} = 9.32^{***}$	$9.4 \pm 9.7^{b,d}$	$1.9 \pm 3.1^{a,c}$	$7.1 \pm 5.1^{b,d}$	$1.5 \pm 2.1^{a,c}$
Presence of current comorbidities, yes/no	$\chi^2_3 = 0.69$	18/3	--	26/8	--

Note.

^{a}Significantly different from *PENK* C-allele carrier cocaine participants

^{b}significantly different from *PENK* T/T cocaine participants

^{c}significantly different from *PENK* C-allele carrier control participants

^{d}significantly different from *PENK* T/T control participants; all variables that differed between the groups were covaried in all analyses.

Behav Brain Res. Author manuscript; available in PMC 2016 October 15.

Table 2

Drug use information of all study participants.

		***PENK*: C-Allele Carrier**		***PENK*: T/T Genotype**	
	Between-Group Test	**Cocaine (n = 21)**	**Control (n =15)**	**Cocaine (n = 34)**	**Control (n = 22)**
Age at onset of cocaine use	$F_{1,52} = 0.02$	24.7 ± 6.9	--	24.48 ± 6.2	--
Duration of cocaine use, years	$F_{1,51} = 1.83$	14.7 ± 8.8	--	17.6 ± 6.7	--
Cocaine urine status, positive/negative	$\chi^2_1 = 0.22$	10/11	--	14/20	--
Use frequency (days/week: last 30 d[e]	$F_{1,51} = 1.22$	3.1 ± 2.8	--	2.3 ± 2.0	--
Current use in $ per use (minimum- maximum, median): last 30 d[e]	$F_{1,47} = 0.45$	0–200, 30	--	0–300, 50	--
Duration of current abstinence, days (minimum-maximum, median)	$F_{1,52} = 0.04$	0–210, 4	--	0–189, 4	--
Score (0–126) on Cocaine Selective Severity Assessment Scale (withdrawal symptoms)	$F_{1,52} = 0.27$	14.1 ± 10.9	--	15.6 ± 10.1	--
Severity of Dependence Scale, 0–15	$F_{1,51} = 0.63$	6.5 ± 4.3	--	7.4 ± 3.7	--
Cocaine Craving Questionnaire, 0–45	$F_{1,53} = 0.04$	15.2 ± 10.1	--	15.9 ± 12.9	--
Current cigarette smoker, yes/no	$\chi^2_3 = 28.20$***	15/6[b,d]	2/13[a,c]	20/14[b,d]	2/20[a,c]
Cigarettes per day, for current smokers	$F_{3,35} = 0.58$	7.0 ± 5.3	4.9 ± 3.5	5.8 ± 4.5	10.5 ± 10.6
Past (heaviest) cigarette use, for current smokers	$F_{3,35} = 0.18$	9.3 ± 6.0	8.5 ± 2.1	8.1 ± 5.8	10.5 ± 10.6
History of alcohol use to intoxication, no/yes[f]	$\chi^2_3 = 20.59$***	11/8[c,d]	8/6[d]	9/24[a,d]	16/1[a,b,c]
Alcohol intoxication days, past 30 days, for those with history of use	$F_{3,35} = 1.36$	0.3 ± 0.7	0.7 ± 1.2	2.1 ± 6.0	10.0 ± 0.0
Alcohol intoxication years, for those with history of use	$F_{3,35} = 1.10$	8.0 ± 6.3	10.3 ± 13.0	11.9 ± 8.5	24.0 ± 0.0
History of cannabis use, no/yes[g]	$\chi^2_3 = 17.81$***	7/13[d]	9/4[c]	10/23[b,d]	14/2[a,c]
Cannabis use days, past 30 days, for those with history of use	$F_{3,38} = 0.17$	0.1 ± 0.3	0.0 ± 0.0	0.1 ± 0.3	0.0 ± 0.0
Cannabis use years, for those with history of use	$F_{3,38} = 2.25$	13.9 ± 8.4	3.8 ± 2.8	12.2 ± 8.0	5.0 ± 5.7

Note.

[a] Significantly different from *PENK* C-allele carrier cocaine participants

[b] significantly different from *PENK* C-allele carrier control participants

[c] significantly different from *PENK* T/T cocaine participants

[d] significantly different from *PENK* T/T control participants

[e] included in brain-behavior correlation analyses

[f] data missing from 3 cocaine participants and 6 controls

[g] data missing from 2 cocaine participants and 8 controls.

Table 3

Main- and interaction effects of *PENK* on brain function and structure.

Region	BA	Side	Voxels	Peak T	Peak P	x	y	z
fMRI: Error>Correct								
C-allele > TT genotype								
Superior Frontal Gyrus	46	L	32	3.38	0.001	−24	50	22
TT genotype > C-allele								
Insula	13	R	51	3.62	<0.001	39	2	7
PENK × Diagnosis Interaction								
Putamen	--	R	48	4.04	<0.001	30	−4	−8
rACC/mOFC	32,10	L	26	3.31	0.001	−9	53	−2
IFG/DLPFC	46,47	R	34	3.05	0.002	36 36	47 44	19 −2
fMRI: Incongruent>Congruent								
C-allele > TT genotype								
Hippocampus/Parahippocampus	30	R	64	4.21	<0.001	21	−25	−11
Insula	13	R	38	4.15	<0.001	45 45	14 17	−11 −2
Postcentral Gyrus	3	L	79	3.47	<0.001	−42	−22	37
Precentral Gyrus	6	L	29	3.45	<0.001	−24	−13	67
Supplementary Motor Area	6	M	56	3.33	0.001	3 0	29 5	61 67
TT genotype > C-allele								
Cerebellum (Vermis)	--	M	39	3.81	<0.001	0	−49	−26
Middle/Superior Temporal Gyrus	21,22	L	45	3.54	<0.001	−51 −51	−4 −7	−17 −5
Thalamus	--	R	46	3.63	<0.001	18	−16	1
Calcarine Fissure	17	L	37	3.59	<0.001	−12	−82	7
Thalamus	--	L	94	3.50	<0.001	−18	−13	−2
PENK × Diagnosis Interaction								
None								
VBM: Gray Matter Volume								
C-allele > TT genotype								

Region	BA	Side	Voxels	Peak T	Peak P	x	y	z
None								
TT genotype > C-allele								
Inferior Temporal Gyrus	37	R	66	3.54	<0.001	48	−51	−9
PENK × Diagnosis Interaction								
Middle Occipital Gyrus	19	L	23	2.89	0.002	−27	−81	42
Middle Temporal Gyrus	37	R	23	2.80	0.003	44	−55	10
Inferior Frontal Gyrus	45	R	17	2.69	0.004	50	32	18

Note. Analyses are one-way ANCOVAs (controlling for variables that significantly differed between the groups as displayed in Table 1); rACC/mOFC=rostral anterior cingulate cortex/medial orbitofrontal cortex; IFG/DLPFC=inferior frontal gyrus/dorsolateral prefrontal cortex; BA=Brodmann Area; R=right, L=left, M=medial; fMRI=functional magnetic resonance imaging; VBM=voxel-based morphometry.